

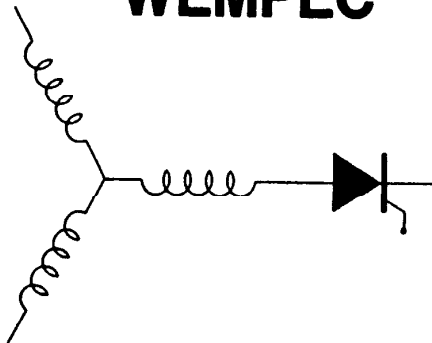
Wisconsin Electric Machines and Power Electronics Consortium

RESEARCH REPORT
90-20

Modelling Saturated AC Machines Via Airgap Flux Harmonic components

J. Moreira, T.A. Lipo
Dept. of Elec. and Comp. Eng.
University of Wisconsin-Madison
1415 Johnson Drive
Madison, WI 53706-1691

WEMPEC



Department of Electrical and Computer Engineering
1415 Johnson Drive
Madison, Wisconsin 53706

©

1990 Confidential

MODELLING OF SATURATED AC MACHINES INCLUDING AIR GAP FLUX HARMONIC COMPONENTS

Julio C. Moreira and Thomas A. Lipo

University of Wisconsin-Madison

1415 Johnson Drive

Madison, WI 53705

Abstract - A new saturation model for induction machines is presented which can be easily extended to other types of ac machines. It is shown that saturation is responsible for the generation of flux space harmonic components travelling in the air gap with the same synchronous speed as the fundamental flux component with the third being the dominant harmonic component. Superposition of the effects of the fundamental and third harmonic components of the air gap flux is utilized in order to model the saturation of the ferromagnetic parts of the machine. The concept of winding functions is used to derive the inductance terms relating both stator and rotor winding components. In this approach the air gap length is assumed to be variable, being a function of the position and level of the air gap flux. Terminal and torque values for steady and transient states are obtainable from the proposed model, with experimental results showing that the model proposed predicts spatial saturation effects with good accuracy.

1. INTRODUCTION

Saturation phenomena in ac electrical machines, especially in induction machines, has received considerable attention in the past few years. In many cases modelling of ac machines under saturation is based on a small signal linearization around an operating point [1]. Another approach proposed in [2] utilizes the concept of reorienting the d - q axis in order to incorporate the effects of spatially dependent saturation into the the main flux path. While the effects of main flux modelling based on the fundamental component of MMF has received much attention, the generation of higher flux harmonics due to saturation has not received the same attention in the literature. The problem of saturation harmonics was first described in [3] wherein the main concerns of the author were the prediction of the air gap flux harmonic component amplitudes and the changes in machine steady state performance. Another approach to determine the air gap flux density harmonic components for induction machines under saturated conditions is described in [4].

In this paper a new saturation model for ac machines is developed based on the fact that the saturation of the magnetic field paths is responsible for introducing harmonic

components of flux due to the non-linear nature of the saturation phenomena. A d - q model is derived from the conventional constant parameters ac machine model, which is modified to account for the saturation. This modification consist in making the air gap length a function of the air gap flux position and amplitude. It is shown that as a consequence of the saturation, a third harmonic flux component exists and third harmonic currents are induced in the rotor circuit. Although of low amplitude, they contribute to the total torque and introduce rotor losses. In addition, the third harmonic of flux when linking the stator windings produces a zero sequence third harmonic voltage component in the stator phases. When the three phase voltages are summed, the fundamental and characteristic harmonics are cancelled and the resultant waveform contains mainly a third harmonic voltage signal which can be used as a means to locating the machine air gap flux [5], [6].

A detailed analytical model is presented and a digital simulation program introduced. The resulting model can be used to predict the dynamic behavior of the machine during transients with large signal variations. Experimental results show that the model proposed predicts the saturation effects with good accuracy.

2. INCORPORATING SATURATION IN THE CONSTANT PARAMETER MODEL

To commence the analysis, it is useful to consider a wye connected three phase ac machine when supplied from a sinusoidal voltage supply. In this case the machine will clearly not have zero sequence harmonic components in the stator current. The air gap flux on the other hand will have present a harmonic content which is a function of the machine saturation. Two different saturation effects must then be distinguished according to the place where the saturation occurs. When saturation occurs in the stator and rotor teeth, the resultant air gap flux assumes a flattened sinusoidal form with a peak value B_g as indicated in Fig. 1.

The resultant air gap flux in Fig. 1 has a harmonic content which includes the all odd harmonic components, including the triplens 3rd, 9th, and so forth. A Fourier series expansion of the air gap flux, however, indicates that the third harmonic is the dominant harmonic component at all

saturation levels. Hence, saturation of the teeth paths can be modelled by the superposition of a third harmonic to the fundamental component of the air gap field flux. It is important to note that this third harmonic flux component travels in the air gap with the same velocity and direction as the fundamental air gap flux component, keeping always the phase synchronism with the fundamental.

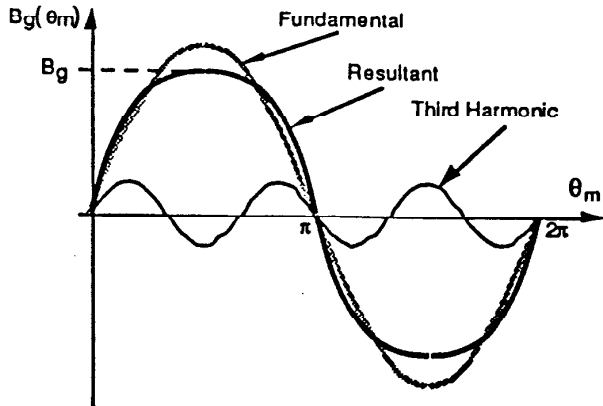


Fig. 1: Air gap flux density distribution for a stator/rotor teeth saturation condition (heavy line). The fundamental and third harmonic components are also shown.

Saturation can also occur at the stator and rotor cores causing also the introduction of harmonic components in the air gap flux. In this case, the core flux distribution assumes a flattened sinusoidal form while the air gap flux distribution assumes a peaked waveform. This peaked air gap flux distribution waveform is explained by the fact that the air gap flux density, $B_g(\theta_m)$, is proportional to the space derivative of the core flux density, $B_c(\theta_m)$. Again, a series of odd harmonics will be present in the air gap flux distribution, but the third harmonic is once again the dominant harmonic component. In this case, the third harmonic has a phase relationship with the fundamental such that one of its peaks enforces the fundamental, giving thus the peaked shape for the resultant air gap flux.

Saturation of the stator and rotor teeth are more common in practical machines since the quantity of iron in the core is much greater than in the teeth, where a much higher flux density exists. Hence, the saturation condition exemplified by Fig. 1 is more typical and will be the case assumed in the analysis throughout this paper.

From the previous paragraphs one can conclude that the presence of third harmonic component in the air gap flux is a sufficient but not a necessary condition for the occurrence of saturation. Both saturation mechanisms have an opposite

effect as third harmonic flux component is concerned. Saturation of the core sections will produce a third harmonic flux component which is in direct phase opposition to the third harmonic produced by the saturation of the teeth paths. Consequently a highly saturated machine do not necessarily have present a high third harmonic flux content.

The third harmonic air gap flux linking the stator spatial winding third harmonic component is responsible for the induction in the stator phases of a zero sequence third harmonic voltage. Since no third harmonic currents will flow in a wye connected machine, this third harmonic voltage keeps the same phase relationship with the flux harmonic and hence can be utilized to locate the air gap field flux with respect to any of the machine terminal quantities. It is important to note that the third harmonic air gap flux component keeps the same zero phase relationship with the fundamental flux for any load condition. This is a direct consequence of the fact that when saturation occurs the air gap flux keeps its flattened sinusoidal form independently on the machine load. It can also be argued in another way by saying that the third harmonic rotor currents are not large enough to produce a rotor mmf which would change the position of the third harmonic flux with respect to the fundamental flux component. This result is of capital importance when control applications as proposed in [5] and [6] utilizing the third harmonic voltage signal are implemented.

Reduction of the magnetic permeability of the iron paths is the immediate consequence of saturation. Figure 2 shows, in a simplified manner, the variation of the stator and rotor iron permeability for a two pole machine. Saturation of the stator and rotor teeth is assumed to occur only in the iron parts with the flux density defined by the resultant component of the air gap flux, B_g . Core saturation regions are also shown in Fig. 2 but for the analysis proposed here only the teeth saturation will be taken into account. This is a reasonable approximation since in most practical machines most of the saturation occurs at the stator and rotor teeth. As the resultant flux B_g moves around the air gap so does the spatial variation of the permeability, suggesting that the permeability variation can be viewed as a travelling wave in the air gap.

We can also recognize that when teeth saturation occurs, the decrease in permeability of the iron paths has the effect of increasing the teeth reluctances for the region around the resultant component of the air gap flux. Keeping, thus, the necessary assumption of constant and infinite iron permeability, the reluctance variation of the teeth can be viewed as an air gap reluctance variation. Since the air gap has a constant permeability (μ_0) the gap length has to be made variable to accommodate the reluctance variation due to the saturation. Therefore, instead of having a variation in the

iron permeability we then assume a pseudo air gap length variation as the flux saturates the iron parts.

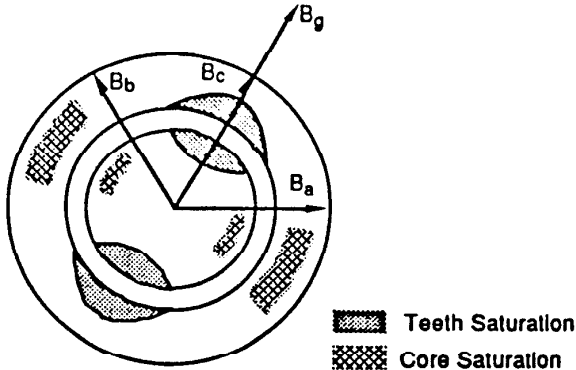


Fig. 2: Cross sectional view of a saturated machine showing the variation of the iron permeability in the stator and rotor parts. Flux density components and the total air gap flux density (B_g) are also shown.

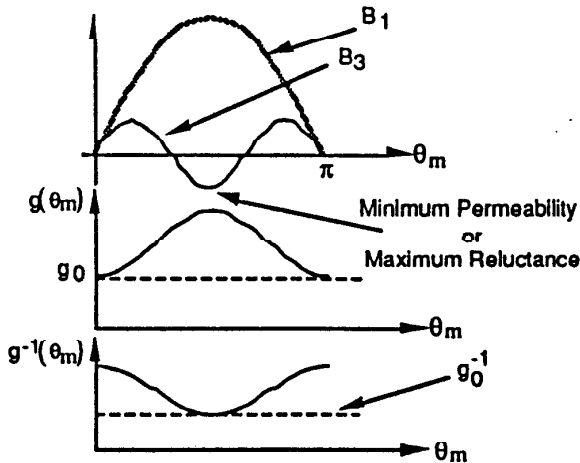


Fig. 3: Air gap length variation function $g(\theta_m)$ and its inverse $g^{-1}(\theta_m)$.

From the discussion in the preceding paragraph it becomes clear that saturation of the stator and rotor teeth can be incorporated into the linear model for the general rotating machine as described in [7] by making the air gap length a function of the saturation level and spatial position. While the air gap length variation is not necessarily a sinusoidal function, it will be assumed so in this analysis. A typical air gap length variation for a pole pitch is shown in Fig. 3

together with its inverse function, $g^{-1}(\theta_m)$. The inverse gap function, $g^{-1}(\theta_m)$, is defined for convenience in dealing with multiplication of functions rather than division, as it would be the case in using $g(\theta_m)$ for computing the inductances of the machine.

As depicted in Fig. 3 an inverse gap function can be defined as

$$g^{-1}(\theta) = k_e + k_m \cos(2\theta_m - 2\theta_f) \quad (1)$$

where

$$k_e = g_0^{-1} - k_m$$

with θ_f representing the position of the air gap flux.

The factor k_m is obtained from the saturation factor for the machine, k_{sat} , as

$$k_m = \frac{1}{2} \frac{k_{sat} - 1}{k_{sat} g_0} \quad (2)$$

with k_{sat} being the ratio between the fundamental components of the air gap voltage for a non-saturated and saturated conditions.

The self and mutual inductances of the stator windings are now computed based on the fact that the air gap length is variable. Based on this approach, winding functions for the stator windings are described as,

$$N_{as}(\theta_m) = N_{s1} \cos\theta_m + N_{s3} \cos 3\theta_m \quad (3)$$

$$N_{bs}(\theta_m) = N_{s1} \cos(\theta_m - 2\pi/3) + N_{s3} \cos 3(\theta_m) \quad (4)$$

$$N_{cs}(\theta_m) = N_{s1} \cos(\theta_m + 2\pi/3) + N_{s3} \cos 3(\theta_m) \quad (5)$$

The self inductance for one of the stator phases, phase a for instance, is computed as,

$$L_a = \frac{\lambda_{aa}}{i_a} = \mu_0 r l \int_0^{2\pi} g^{-1}(\theta_m) [N_{as}(\theta_m)]^2 d\theta_m \quad (6)$$

The mutual inductance between windings of phases a and b , for instance, is computed from

$$L_{ab} = \frac{\lambda_{ab}}{i_b} = \mu_0 r l \int_0^{2\pi} g^{-1}(\theta_m) N_{as}(\theta_m) N_{bs}(\theta_m) d\theta_m \quad (7)$$

The response of the rotor cage to the two components of the air gap flux is a cage current which has two rotating components, one at fundamental and the other at three times the fundamental frequency. Hence, a polyphase fundamental and third harmonic current components are induced in the

rotor creating two components of rotor mmf. It is then necessary to assume that the rotor contains two sets of polyphase winding functions as,

$$N_{ar1} = N_{r1} \cos(\theta_m - \theta_r) \quad (8)$$

$$N_{br1} = N_{r1} \cos(\theta_m - \theta_r - 2\pi/3) \quad (9)$$

$$N_{cr1} = N_{r1} \cos(\theta_m - \theta_r + 2\pi/3) \quad (10)$$

$$N_{ar3} = N_{r1} \cos(3\theta_m - 3\theta_r) \quad (11)$$

$$N_{br3} = N_{r1} \cos(3\theta_m - 3\theta_r - 2\pi/3) \quad (12)$$

$$N_{cr3} = N_{r1} \cos(3\theta_m - 3\theta_r + 2\pi/3) \quad (13)$$

The rotor self and mutual inductances are computed utilizing the winding functions as describe above. These inductance values are organized in two inductance matrixes, one for the fundamental rotor winding function, \bar{L}_{r1} , and other for the third harmonic, \bar{L}_{r3} . These inductances will be time and rotor speed dependent as well as also a function of the saturation factor.

The next step in the modelling of the machine is the derivation of the mutual inductances between the stator and rotor windings. This derivation process leads to two inductance matrixes, \bar{L}_{rs1} and \bar{L}_{rs3} , containing the mutual coupling elements between fundamental and third harmonic components of the rotor and stator windings. These mutual inductances are also time and saturation level dependent.

The abc phase variable machine equations in the vector form are then derived as follows,

$$\bar{v}_{abcs} = \bar{r}_s \bar{i}_{abcs} + \frac{d\bar{\lambda}_{abcs}}{dt} \quad (14)$$

$$\bar{v}_{abcr1} = \bar{r}_{r1} \bar{i}_{abcr1} + \frac{d\bar{\lambda}_{abcr1}}{dt} \quad (15)$$

$$\bar{v}_{abcr3} = \bar{r}_{r3} \bar{i}_{abcr3} + \frac{d\bar{\lambda}_{abcr3}}{dt} \quad (16)$$

The flux linkage equations are written in terms of the stator and rotor current components and the self and mutual inductance matrixes previously defined,

$$\bar{\lambda}_{abcs} = \bar{L}_s \bar{i}_{abcs} + \bar{L}_{sr1} \bar{i}_{abcr1} + \bar{L}_{sr3} \bar{i}_{abcr3} \quad (17)$$

$$\bar{\lambda}_{abcr1} = \bar{L}_{r1} \bar{i}_{abcr1} + \bar{L}_{rs1} \bar{i}_{abcs} \quad (18)$$

$$\bar{\lambda}_{abcr3} = \bar{L}_{r3} \bar{i}_{abcr3} + \bar{L}_{rs3} \bar{i}_{abcs} \quad (19)$$

Note from the flux linkage expressions above that there is no mutual coupling between rotor fundamental and third harmonic windings as expected.

3. SATURATION MODEL IN D-Q-N VARIABLES

The solution for the model derived in Section 2 requires the knowledge of the stator and rotor voltage vectors, \bar{v}_{abcs} , \bar{v}_{abcr1} , and \bar{v}_{abcr3} , since they are the independent variables for the model. The third harmonic component present in these voltages, however, precludes the utilization of them as independent variables for they will be a function of the saturation level of the machine. To circumvent this problem it is necessary to transform the machine equations to the dqn general reference frame. In this new reference system the phase voltages are free from the unknown third harmonic voltage component because these components form a zero sequence set which is eliminated from the dq components of the phase voltages. On the other hand, the n -component of the stator phase voltage is not zero as it is usually the case in the conventional machine model; it contains the third harmonic voltage component which will be solved from the n -axis component of the stator flux. To maintain generality the transformation is carried out in a general reference frame rotating at a speed given by ω .

The machine model in the dqn general reference frame is given by

$$v_{qs} = r_s i_{qs} + \frac{d\lambda_{qs}}{dt} + \omega \lambda_{ds} \quad (20)$$

$$v_{ds} = r_s i_{ds} + \frac{d\lambda_{ds}}{dt} - \omega \lambda_{qs} \quad (21)$$

$$v_{ns} = r_s i_{ns} + \frac{d\lambda_{ns}}{dt} \quad (22)$$

$$v_{qr1} = r_{r1} i_{qr1} + \frac{d\lambda_{qr1}}{dt} + (\omega - \omega_r) \lambda_{dr1} \quad (23)$$

$$v_{dr1} = r_{r1} i_{dr1} + \frac{d\lambda_{dr1}}{dt} - (\omega - \omega_r) \lambda_{qr1} \quad (24)$$

$$v_{nr1} = r_{r1} i_{nr1} + \frac{d\lambda_{nr1}}{dt} \quad (25)$$

$$v_{qr3} = r_{r3} i_{qr3} + \frac{d\lambda_{qr3}}{dt} - 3(\omega - \omega_r) \lambda_{dr3} \quad (26)$$

$$v_{dr3} = r_{r3} i_{dr3} + \frac{d\lambda_{dr3}}{dt} + 3(\omega - \omega_r) \lambda_{qr3} \quad (27)$$

$$v_{nr3} = r_{r3} i_{nr3} + \frac{d\lambda_{nr3}}{dt} \quad (28)$$

where the rotor primed variables are referred to the stator by a stator/rotor turns ratio transformation. For a wye connected stator no zero sequence currents will circulate and consequently i_{ns} is zero, and the same can be assume for the rotor currents i_{nr1} , and i_{nr3} .

The flux linkages in the dqn stator frame are derived after a long algebraic process as,

$$\lambda_{qs} = \left[L_{ls} + L_{m1} + \frac{L_{m1} k_m}{2 k_e} \cos 2(\theta_f - \theta) \right] i_{qs} - \frac{L_{m1} k_m}{2 k_e} \sin 2(\theta_f - \theta) i_{ds} + \left[L_{m1} + \frac{L_{m1} k_m}{2 k_e} \cos 2(\theta_f - \theta) \right] i_{qr1} - \frac{L_{m1} k_m}{2 k_e} \sin 2(\theta_f - \theta) i_{dr1} + L_{s13} \cos 2(\theta_f - \theta) i_{qr3} - L_{s13} \sin 2(\theta_f - \theta) i_{dr3} \quad (29)$$

$$\lambda_{ds} = \left[L_{ls} + L_{m1} - \frac{L_{m1} k_m}{2 k_e} \cos 2(\theta_f - \theta) \right] i_{ds} - \frac{L_{m1} k_m}{2 k_e} \sin 2(\theta_f - \theta) i_{qs} + \left[L_{m1} - \frac{L_{m1} k_m}{2 k_e} \cos 2(\theta_f - \theta) \right] i_{dr1} - \frac{L_{m1} k_m}{2 k_e} \sin 2(\theta_f - \theta) i_{qr1} + L_{s13} \cos 2(\theta_f - \theta) i_{dr3} + L_{s13} \sin 2(\theta_f - \theta) i_{qr3} \quad (30)$$

$$\lambda_{ns} = \sqrt{2} L_{s13} \cos(2\theta_f + \theta) i_{qs} + \sqrt{2} L_{s13} \sin(2\theta_f + \theta) i_{ds} + \sqrt{2} L_{s13} \cos(2\theta_f + \theta) i_{qr1} + \sqrt{2} L_{s13} \sin(2\theta_f + \theta) i_{dr1} - \sqrt{2} L_{m3} \cos 3\theta i_{qr3} - \sqrt{2} L_{m3} \sin 3\theta i_{dr3} \quad (31)$$

Similar flux linkage equations are obtained for the two rotor circuits. It is clear from the preceding Eqs. 29 to 31 that the flux linkages for the d and q -axis components do not result in decoupling between the d - q axis variables as in the conventional model. The machine saturation is responsible for the loss of the decoupling between variables as well as for the generation of the zero sequence flux component, λ_{ns} . The model is greatly simplified by making $\theta = \theta_f$ when the general rotating d - q axes rotate synchronously with the air gap flux. By doing so the cross coupling between the d - q variables observed in the equations above is eliminated. On the other hand, the zero sequence flux linkage still depends on all stator and rotor current components.

The torque produced by the machine is computed from the mutual inductance terms and stator and rotor currents as in [7]. Two torque components arise from this computation process. One of these components is related to the interaction between the fundamental stator and rotor current components, while the other torque term is related to the interaction between the fundamental stator and third harmonic rotor currents. The expressions for these two torque components are given by Eqs. 32 and 33.

$$T_{e1} = \left(\frac{P}{2} \right) \left(\frac{3}{2} \right) \left(L_{m1} - L_{m1} \frac{k_m}{k_e} \right) \left(i_{qs}^e i_{dr1}^{e'} - i_{ds}^e i_{qr1}^{e'} \right) \quad (32)$$

$$T_{e3} = \left(\frac{P}{2} \right) \left(\frac{9}{2} \right) L_{s13} \left(i_{qs}^e i_{dr3}^{e'} - i_{ds}^e i_{qr3}^{e'} \right) \quad (33)$$

The effects of saturation on the torque production mechanism is clearly shown by the torque expressions above. As expected, as the saturation level increases the torque due to the interaction of the fundamental stator and rotor current components decreases. It is interesting to note that saturation is responsible also for the induction of third harmonic currents which will produce a third harmonic rotor flux component. These harmonic rotor currents interact with the stator fundamental current via the pseudo air gap length variation giving rise to the torque component in Eq. 33, which is normally very small compared to the torque produced by the fundamental components. These harmonic rotor currents are also responsible for extra copper losses in the rotor.

The inductance term L_{m1} corresponds to the unsaturated value of the magnetizing inductance which is experimentally obtained. The other inductance terms are given in terms of the machine design parameters.

As in reference [2], the resulting model is dependent on the air gap flux position defined as θ_f . Consequently, the d - q - n variable transformation is performed with respect to this position, when the general argument, θ , becomes θ_f . A

similar technique as in [2] to orient the rotating $d-q$ frame with respect to the air gap flux is used in the implementation of the simulation model.

4. EXPERIMENTAL AND SIMULATION RESULTS

A 3 HP, 230 V, 4 pole induction machine has been instrumented in order to evaluate the correlation between experimental and theoretical results from the model described. All the experimental tests and simulation results were obtained with the machine excited from a sinusoidal voltage supply.

The machine electrical parameters were obtained via the conventional no load and locked rotor tests. Some of the machine design parameters like number of turns for the stator windings, and the number of rotor bars are need for evaluation of the inductance coefficients used in the model.

The no-load characteristic curve (stator line rms voltage versus stator rms current) is measured in the laboratory and is plotted in Fig. 4. The no-load characteristic curve obtained from the saturation model is plotted in the same figure. It is clear that the model predicts the saturation with very good accuracy. In general, the proposed model predicts less magnetizing current, what is an indication that higher harmonic components of the air gap flux contribute to the saturation of the machine. The inclusion of these higher harmonic components of flux will considerably increase the complexity of the saturation model with very little improvement in the final result.

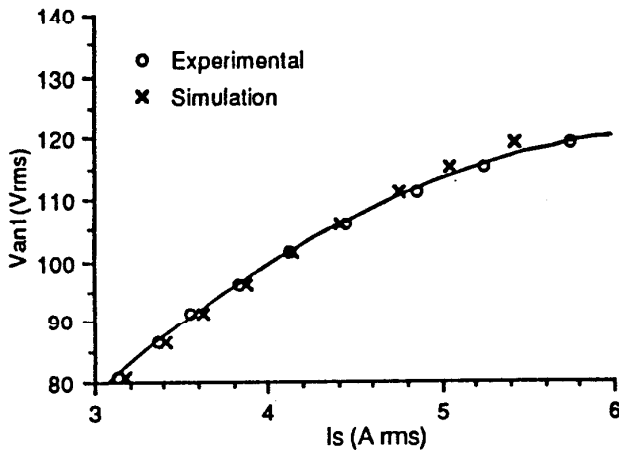


Fig. 4: Magnetization characteristic curve for the induction motor measured experimentally and as predicted by the saturation model.

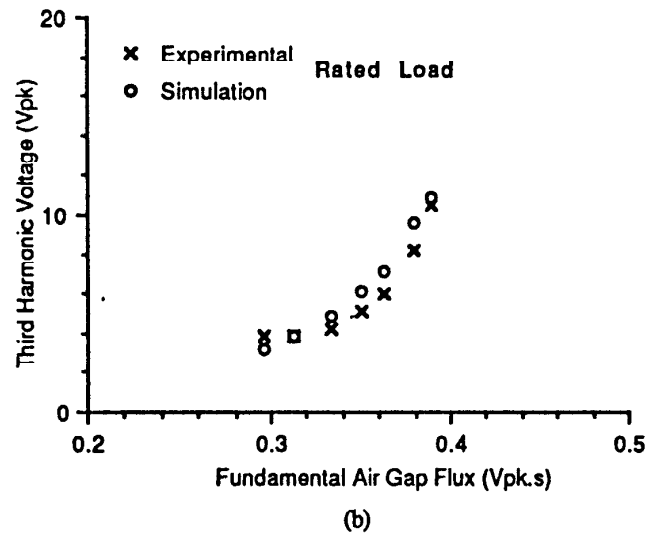
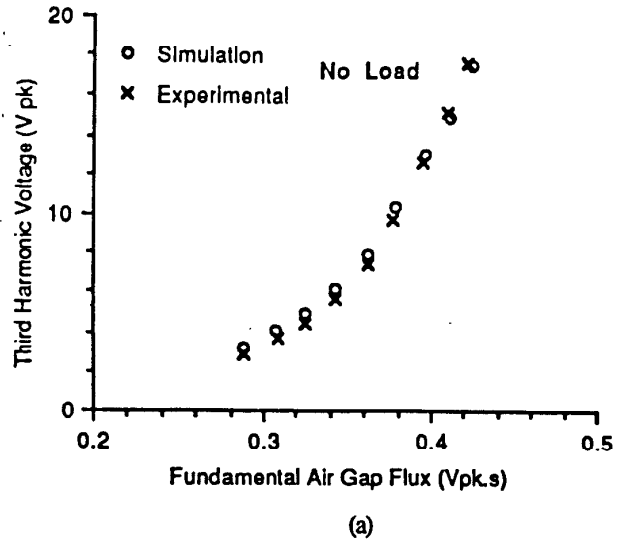


Fig. 5: Amplitude of the stator third harmonic voltage signal as a function of the amplitude of the fundamental component of the air gap flux. Simulation and experimental results are shown for: no load, and rated load conditions.

Figure 5 shows the experimental and simulation results for the amplitude of the stator third harmonic voltage signal as a function of the amplitude of the air gap flux fundamental component for different motor mechanical load conditions. Again good correlation between experimental and theoretical results shows that this saturation model predicts with accuracy the third harmonic component generated by saturation. Note that the third harmonic voltage signal is of

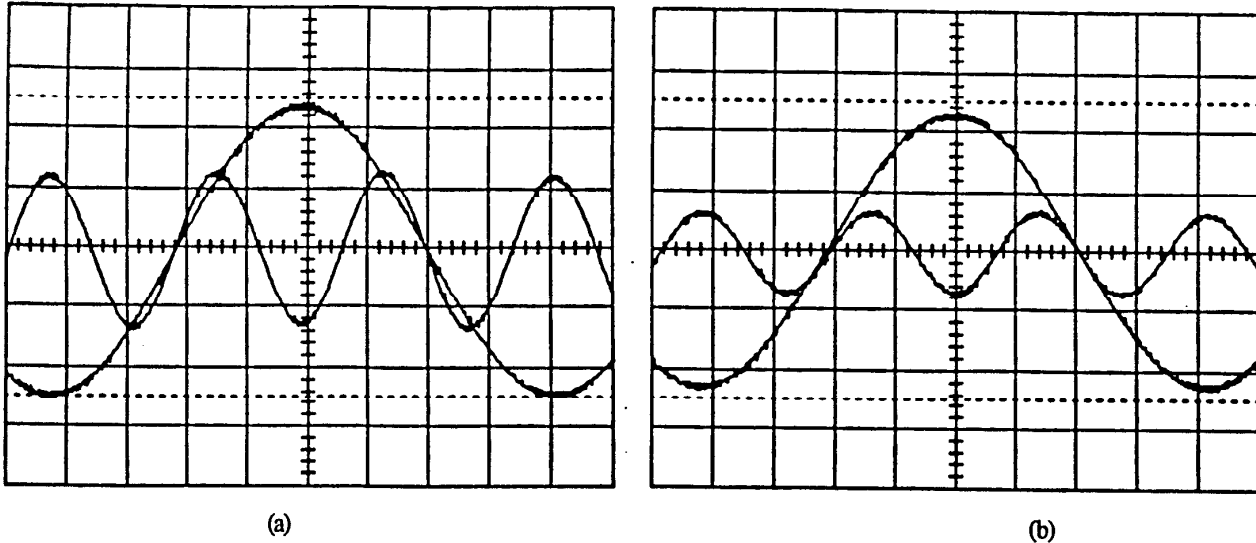


Fig. 6: Fundamental and third harmonic components of the air gap flux for conditions of no load (a), and rated load (b). Scales: fundamental flux- 0.2 V.s/div; third harmonic flux- $5 \cdot 10^{-3}$ V.s/div ; time- $2 \cdot 10^{-3}$ s/div.

substantial magnitude even for flux levels around 60% of the rated value. Consequently, the third harmonic voltage signal will be present even when the machine operates in the field weakening region.

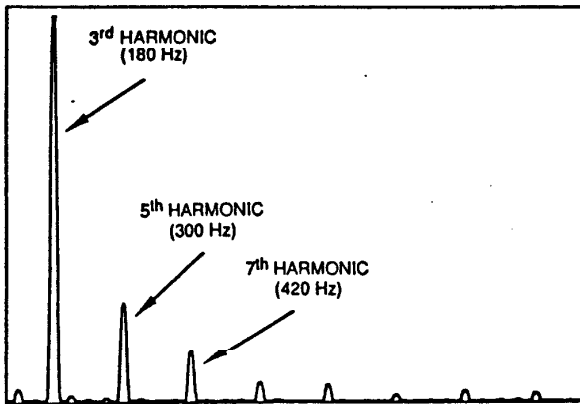


Fig. 7: Frequency spectrum for the air gap flux showing that the third harmonic is the dominant component. Scales: $6 \cdot 10^{-3}$ V.s full scale, 1100 Hz full scale

Figure 6 shows the fundamental and the third harmonic components of air gap flux measured by a search coil installed in the air gap of the machine. These plots are

obtained for no-load and rated load conditions at rated voltage. Note that, as predicted by the model, the loading of the machine does not interfere with the phase relationship between the two flux components. This comes from the fact that the third harmonic rotor currents are very small so that the rotor third harmonic mmf is not large enough to change flattened shape of the air gap flux. Simulation results have shown that the rotor third harmonic currents have values lower than 1% of the rated stator current.

Finally, Fig. 7 depicts the frequency spectrum of the air gap flux density, measured by means of a search coil introduced in the air gap, for the induction machine running at no-load condition. As predicted, the third harmonic is larger than the other harmonics, justifying, thus, the assumption made that it is the dominating harmonic component.

5. CONCLUSION

A new saturation model for induction machine including the effect of third harmonic spatial saturation has been developed and presented in this paper. The model is derived from conventional constant parameter ac machine model modified to account for the stator and rotor teeth saturation effects. It can be used to predict the dynamic behavior of the machine for large signal variations. The model is based on the fact that saturation introduces harmonic components in the air gap flux with the third being the dominant harmonic component. A pseudo variation of

the air gap length is assumed to account for the modulation of the fundamental air gap flux by the third harmonic component. The resultant model contains time varying inductance coefficients which are also a function of the saturation level represented by the saturation factor k_{sat} . It is shown that the rotating third harmonic air gap flux component is responsible by induction of a zero sequence third harmonic stator phase voltage which can be utilized as a means to locate the air gap flux as described in references [5] and [6].

6. INDUCTION MOTOR PARAMETERS

Quantity	Symbol	Value
Line Voltage	V_l	230 V rms
Output Power	P_o	3.0 HP
Speed	ω_r	1740 rpm
Poles	P	4
Stator resistance	r_s	1.11 Ω
Rotor resistance	r_r	0.47 Ω
Stator leakage reactance	X_{ls}	1.05 Ω
Rotor leakage reactance	X_{lr}	1.05 Ω
Unsat. magnet. reactance	X_m	22.09 Ω
Rotor Inertia	J_m	0.0104 Kg-m ²
Number of rotor slots	n_r	46
Number of stator slots	n_s	36
Rotor skew	-	1 slot
Stator pole pitch	τ_s	7/9
Load Inertia	J_L	0.0200 Kg-m ²

7. REFERENCES

- [1] J.A.A. Melkebeek and D.W. Novotny, "The Influence of Saturation on Induction Machine Drive Dynamics", *IEEE Trans. on Industry Applications*, Vol. IA-19, No. 5, September/October 1983, pp. 671-681.
- [2] Y. He and T.A. Lipo, "Computer Simulation of An Induction Machine with Spatially Dependent Saturation", *IEEE Trans. on Power Apparatus and Systems*, Vol. 103, No. 4, April 1984, pp. 707-714.
- [3] C.H. Lee, "Saturation Harmonics of Polyphase Induction Machines", *Trans. AIEE*, Vol. 80, October 1961, pp. 597-603.
- [4] B.J. Chalmers and R. Dodgson, "Waveshapes of Flux Density in Polyphase Induction Motors Under Saturated Conditions", *IEEE Trans. on Power Apparatus and*

Systems, Vol-90, No. 2, March/April 1971, pp. 564-569.

- [5] J.C. Moreira, T.A. Lipo and V. Blasko, "Low Cost Efficiency Maximizer for an Induction Motor Drive", *1989 IEEE Industry Applications Soc. Annual Meeting*, October 1989. (Accepted for Publication in the *IEEE Trans. on Industry Applications*).
- [6] J.C. Moreira and T.A. Lipo, "A New Method for Rotor Time Constant Tuning in Indirect Field Oriented Control", *1990 IEEE Power Electronics Specialists Conference*, June 10-15, 1990, San Antonio, Texas.
- [7] N.L. Schmitz and D.W. Novotny, "Introductory Electromechanics", *book*, Ronald Press, New York, 1965.